Journal of Materials Chemistry A

Accepted Manuscript

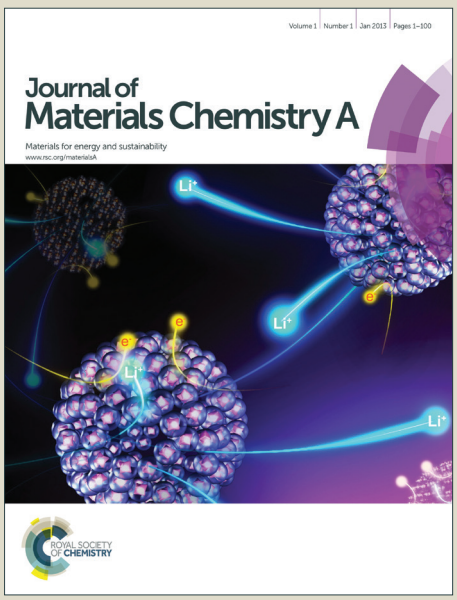

ROYAL SOCIETY OF CHEMISTRY

www.rsc.org/materialsA

Journal of Materials Chemistry A

ARTICLE TYPE

Cite this: DOI: 10.1039/c0xx00000x

www.rsc.org/xxxxxx

Enhanced Photovoltaic Performance with Co-Sensitization of Quantum Dots and an Organic Dye in Dye-Sensitized Solar Cells

Camilla Lelii,[a] Moungi G. Bawendi,*[b] Paolo Biagini,*[c] Po-Yen Chen,[d] Marcello Crucianelli,[a] Julio M. D'Arcy,[d] Francesco De Angelis,[a] Paula T. Hammond*[d] and Riccardo Po[c]

Received (in XXX, XXX) Xth XXXXXXXXX 20XX, Accepted Xth XXXXXXXXX 20XX
DOI: 10.1039/b000000x

CdSe quantum dots of two different sizes, exhibiting a maximum emission at 495 nm ($CdSe_{495}$) and 545 nm ($CdSe_{545}$) were combined with di-tetrabutylammonium cis-bis(isothiocyanato)bis(2,2-bipyridyl-4,4-dicarboxylato)ruthenium(II) (N719) or 2-cyano-3-{5-[7-(4-diphenylamino-phenyl)benzo[1,2,5]thiadiazol-4-yl]-thiophen-2-yl}-acrylic acid (TBTCA) resulting in four novel hybrid organic-inorganic sensitizers, which were used in the fabrication of dye-sensitized solar cells. Results showed that with N719, both CdSe dots decreased the power conversion efficiencies when compared to a standard device consisting only of N719 as sensitizer. With the organic dye TBTCA, $CdSe_{545}$ showed no significant effect, while $CdSe_{495}$ interacted favorably, leading to a 25% increase in power conversion efficiency compared to a device sensitized solely by TBTCA. Studies on excited-states lifetimes of N719 in the presence of CdSe did not distinguish between energy and/or charge transfer mechanisms. On the other hand, time correlated single photon counting experiments onto the photoelectrodes suggest that the advantages due to the $CdSe_{495}$ - TBTCA combination could be ascribed to FRET from quantum dots to the organic dye and to a further contribution, as suggested by IPCE spectra, consisting of electron transfer via cascade from LUMO level of TBTCA to $CdSe_{495}$ to TiO_2, that produces a higher flux of electrons in the external circuit.

Introduction

The worldwide energy demand is dramatically increasing, and primary energy sources are derived from carbon-based fossil fuel. 90% of greenhouse gas emissions come from the combustion of fossil fuels, leading to serious climate change. The lack of clean energy motivates scientists to find alternative and eco-friendly energy sources and therefore solar energy is an ideal candidate because it is clean and freely available.[1-3] Harvesting energy from the sun can be accomplished via inorganic solar cells such as single crystal silicon, polycrystalline silicon, and copper indium gallium selenide, as well as via organic technologies such as bulk heterojunction, bilayered, and dye-sensitized solar cells (DSSCs). Among these photovoltaics, DSSCs have attracted considerable attention due to an ideal compromise between efficiency and cost-performance.[4-6] The photoanode of DSSC is comprised of a nanoporous TiO_2 layer sensitized by photosensitizers which is commonly considered a crucial part in this kind of devices. Ideally the photosensitizer might absorb energy both in the whole visible region and in the near-infrared (NIR) moreover its excited state should be at higher energy level than the conduction band of the semiconductor to facilitate electron injection. However, the traditional dyes generally used in DSSCs suffer from narrow absorption spectra and/or low molar extinction coefficients,[5] so a new approach has emerged, that further improves the efficiency, by co-sensitizing dyes with small band gap semiconductor nanocrystals (QDs). In fact, QDs preserve advantages, such as high molar extinction coefficients and large intrinsic dipole moment, furthermore quantum confinement and a tunable band gap, dependent on the size and shape of QDs, enables designing light-absorbing materials with tailored optical properties.[7-9] These peculiar characteristics can be exploited in co-sensitized devices, where QDs play an important role in charge and/or energy transfer processes.[10] The advantages of the co-sensitization are several: (i) the problems arising from internal recombination of QDs can be overcome thanks to the capability of the dye that works as hole scavenger, leading to a better charges separation and higher electron injection yields;[9] moreover (ii) tuning the optical properties of the dots according to the dye affords the possibility for increasing light absorption in order to match the solar spectrum;[10] finally (iii) by combining QDs and dye the interaction between them can lead to FRET (Förster Resonance Energy Transfer) processes, where the former can act as donor and the latter as acceptor thereby enhancing cell efficiency. In

this way common dyes for DSSCs with good charge injection ability but with narrow absorption spectra or low molar extinction coefficients, now can serve as efficient sensitizers.[5,11]

Previous studies have focused on the interactions between semiconductor nanocrystals and dyes[12-21] as well as the charge transfer processes.[9,22-33] Wang and Liu[26] reported co-sensitization with N719 and PbS quantum dots and they obtained an increasing of efficiency from 5.95%, of device sensitized only with N719, to 6.35% in the co-sensitized device. Moreover Song et al.[28] built the photoanode of the solar cells using ZnO nanowires coated with CdS quantum dots and cis-bis(isothiocyanato)bis(2,2-bipyridyl-4,4'-dicarboxylic acid)ruthenium(II) (N3) dye reporting a conversion efficiency enhanced from 0.5% of N3 sensitizer to 1.9% of co-sensitizer and attributing this improvement to an efficient hole transfer from CdS to N3 that avoids the exciton recombination inside the QDs and ensures the electron injection into ZnO nanowires. Many advantages have been obtained using CdSe or CdS nanocrystals and squaraine dyes that absorb selectively in NIR region[34] and can work as an acceptor of both holes and energy via FRET deriving from QDs. For example Kamat et al.[20] proved a profitable energy transfer from CdSe to squaraine dye that enhanced the efficiency of the devices from 3.05% in DSSC to 3.65% in QDDSSC. Another important result was obtained by Etgar et co-workers[21] that enhanced the power conversion efficiency by 47% due to FRET from CdSe quantum dots to the squaraine dye. Despite considerable improvement, the overall efficiency of devices sensitized with squaraine dyes and QDs is still rather low,[20,21,30] these devices use electrolytes based on cobalt or sulfide/polysulfide redox couples. Even though the mentioned redox couples have shown to be, in QDs-based devices, more suitable than traditional I^-/I_3^- based electrolytes, the iodide couple remains a good choice for DSSCs because it is a good regenerator of the oxidized state of the dye and minimizes the recombination of the electrons of TiO_2 with electrolyte acceptors.[5] Only in few cases traditional push-pull organic dyes, perceived as more efficient than squaraine, have been employed together with QDs.[27,29,33] Fan and co-workers[29] reached a very good increasing using QDs together with 2-cyano-3-(5-(9-(4-(2,2-diphenylvinyl)phenyl)carbazol-6-yl)thiophen-2-yl)-acrylic acid (JK28) passing from efficiency of 0.41% in the devices sensitized with JK28 only to 1.03% in co-sensitized device and recently Hua[33] obtained an efficiency up to 7.20% in a co-sensitized device based on $CuInS_2$ QD and 2-cyano-3-(5-(5'-(5-(4-(diphenylamino)phenyl)thiophen-2-yl)-4,4'-dihexyl-2,2'-bithiazol-5-yl)furan-2-yl)acrylic acid (BTF), with an increase around 7% with respect to the corresponding device without QDs. Here we describe devices using iodide-based electrolytes and shed light on the conditions in which co-sensitization between organic dye (TBTCA) and CdSe QDs can realize and the achieved increase around 25% represents, to the best of our knowledge, the top augment for a device based on push-pull organic dye, QD and I_2/I_3^- redox couple; by comparison we also report the attempts to obtain, in the same conditions, co-sensitization between the same CdSe QDs and N719 dye.

Experimental

Measurements

The cyclovoltammetric (CV) characterization was carried out using an Autolab PGSTAT 12 potentiostat/galvanostat (EcoChemie, The Netherlands) run by a PC with GPES software. XPS measurements were performed on a TiO_2 film (5 μm thick) with PHI VersaProbe II XPS instrument. TCSPC measurements were performed with an apparatus composed as follow. Excitation source: Picoquant PDL-800B driver with LDH-C 400 module; 2.5 MHz pulse train; 400 nm center wavelength; ~30 ps pulse duration (estimated); 450 nm short-pass filter (Thor Labs FES0450). Beamsplitter: Pellicle beamsplitter (Thor Labs BP208); Roughly 92% transmission over visible spectrum. Sample objective: 4x Nikon air objective. Emission filter: 500 nm and 600 nm long-pass (Thor Labs FEL0500 and FEL0600). Detection: Perkin-Elmer SPCM (single-photon APD); PicoHarp 300 (timing module). TEM imaging analysis was performed using JEOL JEM-2100F Field Emission Electron Microscope at 200 kV accelerating voltage and illumination angle α=1. CdSe-sensitized TiO2 film was scratched from FTO glass and transferred into a vial containing ethanol (1-2 ml) and sonicated for 5 min. Few drops of this solution were applied on a formvar/carbon coated copper grid 400 mesh and dried in air. Electron Probe Micro Analysis (EPMA) were performed on the QD-sensitized TiO_2 film cross sections with a JXA-8200 Superprobe (JEOL), with an operating Voltage of 15 kV. The film was made by doctor blade technique on a 1 mm sodalime glass substrate. The samples were coated with carbon, using high vacuum carbon evaporator and all measurements were referred to pure element standards.

Synthesis

All reactions were performed using standard glass vessels under an inert nitrogen atmosphere. All the solvents were purchased from Sigma Aldrich and, unless otherwise specified, they have been used without further purification. K_2CO_3 (Carlo Erba), $MgSO_4$ (Carlo Erba), TiO_2 paste, T/SP - 20 nm (Solaronix), N719 (Solaronix), TBTCA was prepared according to a modification of the literature procedures,[35,36] all the other chemicals here employed were acquired from Aldrich and they were all used as received.

Synthesis of $CdSe_{495}$ and $CdSe_{545}$ QDs

Trioctylphosphine oxide, TOPO (3.0 g, 7.8 mmol)), octadecylphosphonic acid, ODPA (0.28 g, 0.84 mmol)) and CdO (0.06 g, 0.47 mmol) were mixed in a 50 ml flask, heated at 150°C and exposed to vacuum for ca. 1 hour. Then, under nitrogen, the solution was heated to about 300°C to dissolve the CdO until it turns optically clear and colorless. At this point, 1.5 g (4.0 mmol) of trioctylphosphine, TOP was injected in the flask and the temperature was allowed to recover to the value required for the injection of the Se:TOP solution [Se (0.058 g, 0.73 mmol) + TOP (0.36 g, 0.97 mmol)]. The injection temperature and the reaction time are modified in order to synthesize CdSe dots of different sizes. As an example, for the synthesis of green fluorescent CdSe dots the Se:TOP solution was injected at 380°C and the heating mantle was removed immediately after the injection. On the other hand, red fluorescent CdSe dots were synthesized by injecting the Se:TOP at 370°C and stopping the reaction heating only after 3 minutes. After the synthesis, the nanocrystals were precipitated with methanol/butanol, they were purified by repeated redissolution in hexane and precipitation with the same mixture of methanol/butanol, and they were finally dissolved in hexane.[37]

Fabrication and Characterization of solar devices

FTO glass (TEC15; thickness, 2.2 mm; 15Ω/square; Pilkington, USA) was first cleaned in a detergent solution using an ultrasonic bath for 15 min, then rinsed with water and ethanol. The FTO glass plates were immersed in a 40 mM aqueous $TiCl_4$ solution at 80°C for 30 min and washed with water and ethanol. A layer of TiO_2 paste was deposited on the FTO glass plates by doctor blade technique and then dried for 5 min at 120°C. This procedure was repeated, if necessary, to achieve an appropriate thickness of 10

μm. After drying at 120°C the film thus produced was sintered at 500°C for 30 min. After cooling at 80°C the film (about 10 μm thick, measured through VEECO Dektak 150 profilometer) was immediately dipped into a 0.5 mM dye solution in the proper solvent (N719 in ethanol and TBTCA in dichloro-methane) for 18 h. For the co-sensitization, the film was first immersed in a 1 μM hexane solution of CdSe QDs for 18 h and then in the aforementioned dye solutions.

The counter-electrode was 100-nm-thick platinum, sputtered on an ITO glass (Delta Technologies). A solution 0.6 M of 1-butyl-3-methylimidazolium iodide, 0.03 M of I_2, 0.10 M of guanidinium thiocyanate and 0.5 M of 4-tert-butyl pyridine acetonitrile/valeronitrile (85:15, v:v) has been used as electrolyte. The dye-adsorbed TiO_2 photoanodes and platinum counterelectrodes were assembled into a sandwich-type cell and sealed with a hot-melt Surlyn resin with a thickness of 25 μm (Solaronix). The TiO_2 electrodes had an area of about 0.16 cm^2 . The aperture of the Surlyn frame was larger than that of the TiO_2 area by 2 mm. Copper tape was adhered on the edge of the FTO outside the cell. The position of the tape was 1 mm away from the edge of the Surlyn gasket and 4 mm away from the edge of the TiO_2 layer.

Photovoltaic measurements were performed using an AM 1.5 solar simulator (Photo Emission Tech.). The power of the simulated light was calibrated to 100 mW cm^{-2} by using a reference silicon photodiode with a power meter (1835-C, Newport) and a reference silicon solar cell to reduce the mismatch between the simulated light and AM 1.5. *J–V* curves were obtained by applying an external bias to the cell and measuring the generated photocurrent with a Keithley model 2400 digital source meter. The voltage step and delay time of photocurrent were 10 mV and 40 ms, respectively. IPCE spectra were obtained with a computer-controlled system (Model QEX_7, PV Measurements, Inc.) consisting of 150 W xenon lamp light source and a monochromator with two 1200 g/mm diffraction gratings. The monochromator was incremented through the wavelength range from 350 nm to 900 nm to generate the spectral response of IPCE with a spectral resolution of 10 nm. The incident photon flux was determined using a calibrated silicon photodiode (calibrated by PV Measurements, Inc.). Measurements were performed in a short-circuit condition, while the cell was under background illumination from a bias light of 50 mW cm^{-2}. Bias illumination was from the same direction as the monochromatic light, which was from the FTO side. The monochromatic beam was chopped using a computer-controlled shutter at a frequency of 4 Hz, and averaging of up to 40 shutter cycles was employed.

Results and discussion

Evaluation of coverage of TiO_2 surface by QDs

A crucial point of QDs-sensitized solar cells is the sensitization of TiO_2 with QDs. QDs do not present an anchoring functional group to bind the TiO_2 surface; in addition they are passivated with organic ligands, which make the sensitization on TiO_2 and charge transfer processes across the interfaces complicated. Several approaches to deposit QDs on TiO_2 film are described in literature:[38] Chemical-Bath Deposition (CBD) and Successive Ionic-Layer Adsorption and Reaction (SILAR) are in-situ techniques which are able to provide high surface coverage and intimate contact with wide bandgap semiconductor, facilitating charge injection processes. However, the CBD and SILAR processes lead to a polydisperse size distribution, which affects the band gap of QDs. Otherwise pre-synthesized monodisperse QDs are usually prepared ex-situ and deposited directly or through molecular bifunctional linker onto semiconductor film. In this case, the functional molecular linkers provide a better coverage but they can interfere in charge transfer processes.[39-42] So we thought that by depositing monodisperse QDs directly on TiO_2 film, without any molecular linker, although it is not the optimal method to obtain a complete coverage of TiO_2 layer, is the best method to study their role in the devices, in fact it avoids any interference due to the molecular linker in charge separation processes and to the heterogeneity of the properties of QDs caused by polydisperse size distribution obtained when other in-situ methods (CBD and SILAR) are employed.[38,43]

We have prepared CdSe QDs according to a standard literature procedure[37] which consists in the reaction of a CdO solution, tri-octylphosphine oxide (TOPO) and tri-octylphosphine (TOP) in octadecylphosphonic acid (ODPA) and by means of an accurate control of the tem-perature and of the reaction time with a Se:TOP solution, we were able to easily regulate the dimension of the CdSe QDs, which also keep an elevated uniformity in their size distribution as confirmed by TEM analysis (Fig. 1), while the determination of the corresponding amount in solution was determined by spectroscopic method.[44]

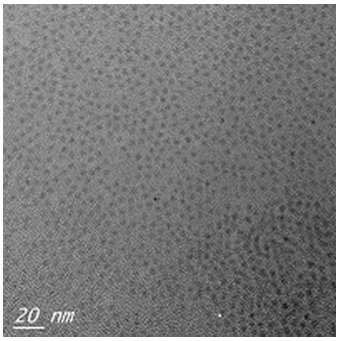

Figure 1. TEM image of CdSe solution in n-hexane.

QDs/TiO_2 films were obtained by prolonged dipping of a TiO_2 film (10 μm thick, sintered on FTO glass) into CdSe QDs solution in hexane (See experimental method section for more details).

To preliminarily assess the uniformity of CdSe dispersion on TiO_2 films, a X-ray Photoelectron Spectroscopy (XPS) characterization of CdSe/TiO_2 composite films (5 μm thick) on the surface and depth profile was carried out. The surface survey, performed on two different spots of the surface, showed an average atomic percentage of cadmium of 5.9 ± 0.4 versus a titanium percentage of 15.1 ± 0.1. Depth profile characterization has been done sput-tering the sample with high energy Ar^+ ions. To correlate the sputtering time to the thickness of the film, we have controlled the disappearance of Ti peak over the sputtering time. The result is that Ti peak disappears after 220 minutes of sputtering and this time corresponds to 5 μm thickness. On the other hand the analysis on the CdSe-TiO_2 composite films reveals that Cd peak disappears after just 5 minutes so we can reasonably assume that CdSe QDs are located in a very thin top layer and considering that 220 min were needed to remove a 5 μm layer of TiO_2 we can assume that CdSe QDs penetrate up only to around 100 nm. (see Supporting Information for more details).

These results can be compared with electron probe micro analysis performed directly on the cross section of the QDs/TiO_2 composite films (10 μm thick) (Fig. 2).

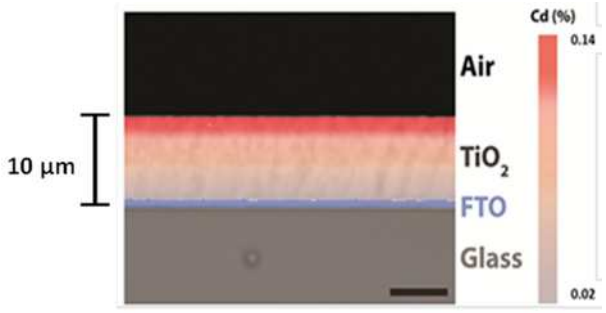

Figure 2. SEM image, performed with electron probe micro analyzer, of the cross-section of the CdSe-sensitized TiO_2 film (10 µm thick) deposited on FTO glass.

The analyzer works similarly to a scanning electron microscope (SEM): the sample is bombarded with an electron beam, emitting x-rays at wavelengths characteristic to the elements being analyzed. This enables to determine the abundances of elements present within small sample volumes (typically 10-30 μm^3 or less).[45]

As we can see from the SEM image of the Electron Micro Probe Analyzer (Fig. 2) the maximum amount of Cd is on the top of the photoanode, and its atomic percentage is estimated to be around 0.14%. This small value may seem apparently inconsistent with the XPS results that indicated 5.9% of Cd atoms, but we confidently consider the value obtained with EMPA, an average in the first 2 µm of the overall thickness since the electron beam used can detect a sample sphere of 2-3 µm in diameter. Complete results of EMPA are reported in Table 1.

Table 1. Atomic concentration at different depth. Analysis performed on the cross section of 10 micron thick TiO2 film sensitized with CdSe by Electron Probe Micro Analysis.

Depth (µm)	Ti %	O %	Cd %	Se %
2	27.8 ± 0.2	71.8 ± 0.8	0.141 ± 0.005	0.198 ± 0.006
4	29.2 ± 0.3	70.6 ± 0.8	0.041 ± 0.004	0.081 ± 0.005
6	29.7 ± 0.3	70.2 ± 0.8	0.025 ± 0.004	0.061 ± 0.005
8	29.1 ± 0.3	70.9 ± 0.8	0.018 ± 0.004	0.057 ± 0.005

Ultimately, considering the results obtained by XPS and EMPA we recovered the following information: (i) the amount of atomic Cd on the top of TiO_2 layer is 5.9%; (ii) QDs are located within around 100 nm thickness of TiO_2 layer; (iii) the mean value of atomic Cd in the upper 2 µm is 0.14%. So we can conclude that, in these conditions CdSe QDs cannot penetrate homogeneously into the whole mesoporous titania structure.

Evaluation of CdSe QDs effects in solar cells

The fabrication of the devices was performed by conventional techniques[46] and are exhaustively described in the experimental methods. We tested two different CdSe QDs: $CdSe_{495}$ and $CdSe_{545}$ (the number refers to the wavelength of maximum of emission), each one with two different dyes: the commercially available ruthenium complex N719 and an already described[35] organic dye (TBTCA), which we prepared according to a partially modified method allowing us to avoid the use of stannyl derivatives[36] (Figure 3).

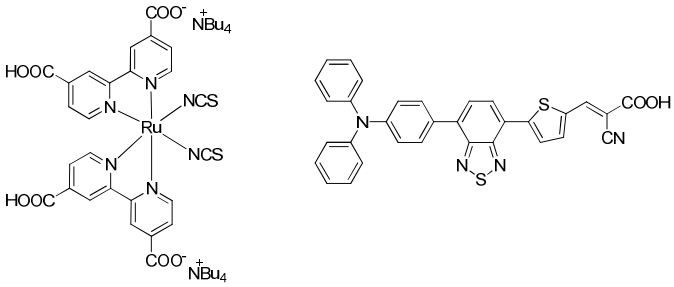

N719 TBTCA

Figure 3. Structure of dyes employed.

The co-sensitized devices (QDDSSCs) were compared with the respective cells assembled with dye alone (DSSCs). In Table 2 are summarized the main photovoltaic parameters measured in the presence of I^-/I_3^- based electrolyte solutions (see experimental methods for more details). In these conditions we didn't observe any decrease in the efficiency for all the devices during the characterizations (*J-V* curves and IPCE), which normally were completed within 3 – 4 h.

Table 2. Photovoltaic parameters of DSSCs and QDDSSCs.

Entry	Sensitizer	J_{SC} mA/cm^2	V_{OC} V	FF %	η %
1	$CdSe_{495}$	0.3	0.62	61	0.1
2	$CdSe_{545}$	0.3	0.65	57	0.1
3	N719	13.5	0.79	71	7.6
4	N719–$CdSe_{495}$	11.6	0.76	75	6.6
5	N719–$CdSe_{545}$	11.1	0.68	74	5.6
6	TBTCA	8.4	0.63	76	4.0
7	TBTCA–$CdSe_{495}$	9.6	0.67	77	5.0
8	TBTCA–$CdSe_{545}$	8.3	0.64	74	3.9

As shown in Table 2, CdSe QDs have different effects on N719 and TBTCA. When CdSe QDs are employed together with N719, they indifferently produced a decrease in the device efficiency. In the literature there are several reports demonstrating that Ru-dye/QD devices work better than Ru dye devices,[47,48] but there are also a few exceptions. For example, Lin et al.[31] attributed the degradation of the performances of a N719/CIGS QD solar cell, compared to a pristine N719 device, to an energy levels misalignment; Mora-Seró et al.[10] ascribed the performance degradation to the existence of new charge recombination channels. When CdSe QDs are used with TBTCA, the efficiency of the co-sensitized device with TBTCA-$CdSe_{495}$ was increased of about 25% (η rise from 4.0% to 5.0%). The enhanced efficiency mainly derived from the improved photocurrent density (J_{SC}). Concerning the open circuit voltage which

corresponds to the difference between Fermi level of TiO_2 and redox potential of I^-/I_3^- couple[5,11] and it can be significantly affected when the wide bandgap semiconductor is in contact with a dye or other materials. In the cases here considered, the V_{oc} is mainly altered by passing from N719 (0.79 V) to TBTCA (0.63 V), while the addition of CdSe QDs to the corresponding DSSCs generated only small variations, negative for N719 and positive in the case of TBTCA. In Figure 4 are reported the J-V curves and the IPCE spectra of all the combinations, between N719 or TBTCA with both types of CdSe QDs, investigated.

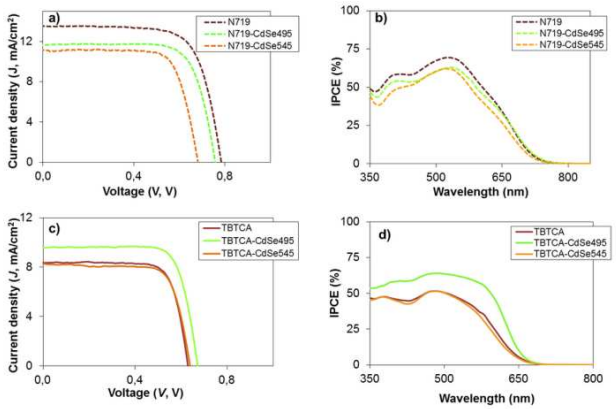

Figure 4. a) Comparison of J-V curves of devices sensitized with N719 alone (dark dotted line) , N719-$CdSe_{495}$ (green dotted line), N719-$CdSe_{545}$ (orange dotted line); **b)** Comparison of IPCE spectra of devices sensitized with N719 alone dark dotted line), N719-$CdSe_{495}$ (green dotted line), N719-$CdSe_{545}$ (orangen dotted line); **c)** Comparison of J-V curves of devices sensitized with TBTCA alone (dark bold line), TBTCA-$CdSe_{495}$ (green bold line), TBTCA-$CdSe_{545}$ (orange bold line); **d)** Comparison of IPCE spectra of devices sensitized with TBTCA alone (dark bold line), TBTCA-$CdSe_{495}$ (green bold line), TBTCA-$CdSe_{545}$ (orange bold line).

The improved efficiency obtained with the combination TBTCA–$CdSe_{495}$ which, as explained above, was essentially due to an increase in the photocurrent density (Figure 3 c), consequently the corresponding IPCE curve (Figure 3d) get to 65%, close to the 500 nm region, starting from about 50% referred to the device sensitized with organic dye TBTCA only. All these evidences suggest that adding $CdSe_{495}$ to TBTCA a surplus of electrons flows through the circuit resulting in an improved performance of the device.

Finally it should be noted that, in the examined conditions, the efficiency of the devices with QD alone were quite low and in all the considered combinations QD/dye we observed a significant improvement of the devices efficiency. This behaviour had already been reported.[20,21,33,49,50] In particular F. Guo[33] ascribed the enhancement to the interaction between QD and dyes (QD formed a barrier layer to suppress the recombination from injection electron to the electrolyte and improve open-circuit voltage). On the other hand the <0.1% efficiency measured for the devices containing only the QD was explained on the basis of a very low light harvesting capability of the QD. However we believe, accordingly to Mora-Seró's observations[9], that the issue arises from the effective internal recombination of QDs, that could be bypassed thanks to the capability of the dye to work as hole scavenger, producing a better charges separation and higher electron injection yields.

Evaluation of excited state lifetimes

To study energy transfer kinetics in our devices, we performed time correlated single photon counting (TCSPC) experiments on the photoanode. The resulting PL lifetime traces are shown in Figure 5.

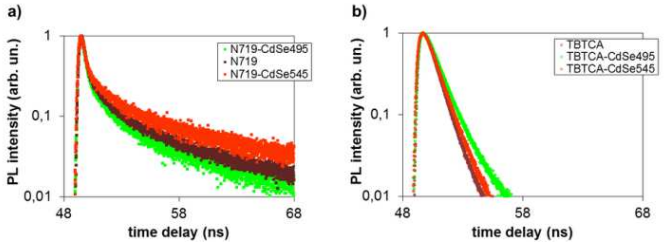

Figure 5. a) Comparison of decay profile between N719 (dark filled squares), N719-$CdSe_{495}$ (green filled squares) and N719-$CdSe_{545}$ (orange filed squares) @TiO_2 film deposited on FTO glass, the PL wavelength detected for the decay profile is around 700 nm; **b)** Comparison of decay profile between TBTCA (dark circles), TBTCA-$CdSe_{495}$ (green circles) and TBTCA-$CdSe_{545}$ (orange circles) @TiO_2 film deposited on FTO glass, the PL wavelength detected for the decay profile is around 680 nm.

We cannot observe marked differences between N719 and N719+CdSe and in both cases the decay profile clearly shows a multiexponential behavior (Fig. 5a) meaning that several competitive decay processes may happen at the same time. In fact, as explained by Mora-Seró et al.,[10] there are different pathways for the photogenerated charge, as shown in Figure 6a, where are schematically proposed the most likely situations for a QDDSSCs in terms of energy levels arrangement.

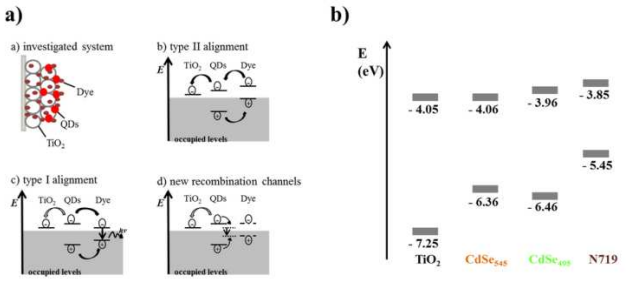

Figure 6. a) Schematic illustration, adapted from the study of Mora-Serò et al.,[10] of possible energy level alignments and related photogenerated-charge-carrier dynamics adapted from ref. 10; **b)** Energy levels alignment N719 and CdSe.

The best case, to produce improvement in the device efficiency, is the type II alignment where there is directional charge separation for both electrons and holes. Otherwise, if the LUMO of the dye is located below the Conduction Band (CB) of the QD, as in the case of type I alignment, directional charge separation will be weakened, the dye can only act as hole scavenger and it could be an increased photoluminescence emission of the dye. Moreover many new recombination channels, internal to the QD, could appear when QDs are combined with other materials.

In our specific case (Fig. 6b) the energy levels values were not determined rigorously, but were recovered on the basis of previous works,[21,51,52] readjusting the band gap of QDs according to their size. The LUMO of N719 results really close to the CB of both $CdSe_{495}$ and $CdSe_{545}$ QDs, so as a matter of fact it could be just a little above or below the CB and relating to the scenery proposed by Mora-Seró[10] can fit even into this case. Furthermore, analyzing the UV-visible spectra (Fig. 7a), FRET (Forstër Resonance Energy Transfer) energy transfer may occur

too, since overlap between the absorption spectrum of N719 and emission spectra of CdSe QDs has been clearly observed. This complicated framework make interpreting the interaction between CdSe QDs and N719 very difficult.

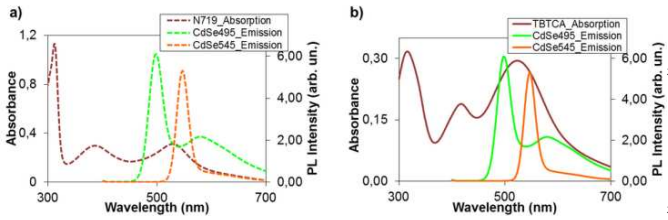

Figure 7. a) Absorption spectra of N719 (dark dotted line), emission spectrum of $CdSe_{495}$ (green dotted line); emission spectrum of $CdSe_{545}$ (orange dotted line); **b)** Absorption spectra of TCBCA (dark bold line), emission spectrum of $CdSe_{495}$ (green bold line),emission spectrum of $CdSe_{545}$ (orange bold line).

The combination of TBTCA with $CdSe_{545}$ did not lead to any remarkable changes in the decay time of the dye, whereas the mixture of $CdSe_{495}$-TBTCA@TiO_2 brings about a well defined slower decay than TBTCA@TiO_2 one, moreover it is possible to roughly fit the decay curve (Fig. 5b) with a monoexponential function, so we can suppose that in this case only one process could preferably operate. These observation are consistent with FRET from $CdSe_{495}$ to TBTCA, that could be the main reason for the increased efficiency in the corresponding devices (Table 2, entry 7). Spectroscopic investigations (Fig. 7b) also suggest the real possibility to have FRET between CdSe QDs and TBTCA. It is worth to note that only $CdSe_{495}$ are characterized by a significant trap emissions (fig. 7a-b) clearly evidenced by the presence of a broadened red-shifted band centered at 580 nm which is closely related to the presence of intra-band states.[53] Moreover, if we look carefully at the IPCE spectrum (Fig. 4d), the increased photocurrent realized around 400 nm can be reasonably ascribed to FRET from $CdSe_{495}$ to TBTCA, which might be more efficient owing to the optimal superimposition between dye absorption and QDs emission bands also assured by the presence of trap emissions, but the improvement evidenced around 600 nm could be attributed to a charge transfer via cascade of electrons from the LUMO of TBTCA to the CB of $CdSe_{495}$ and finally into the TiO_2 semiconductor (Fig. 8).

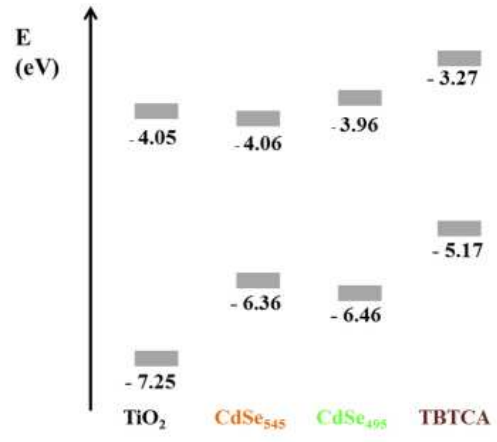

Figure 8. Energy levels alignment of TBTCA and CdSe QDs.

Figure 8 shows the energy levels scheme of the sensitizers. In this case the energy levels of TBTCA are experimentally determined by cyclovoltammetric measurements on a film generated from 1,2-dichlorobenzene solution, whereas TiO_2, $CdSe_{545}$ and $CdSe_{495}$ levels are recovered from the literature.[51,52] The experimental data of devices suggest that only $CdSe_{495}$ owns the right energy levels to ensure the proper alignment between TiO_2, and TBTCA that allows a further driving force to the electrons to be injected into the CB of the TiO_2 and on the basis of these observations it is possible to explain the different behavior of the two CdSe QDs samples observed in the corresponding QDDSSCs devices. Lastly, although TCSPC experiments reveal some physical-chemical processes involved between the constituents of the photoanode in open circuit conditions, the IPCE measurements provide the evidences of a more complicated system and by intersecting all the experimental results, it is possible to attribute the enhancing efficiency of TBTCA-$CdSe_{495}$-Sensitized Solar Cells to either energy and charge transfers.

Conclusions

In this work we studied the effects of the co-sensitization of TiO_2 with CdSe QDs and dye. Firstly we characterized qualitatively and quantitatively the CdSe-sensitized titania film showing that QDs do not penetrate completely into the mesoporous TiO_2 film but they are just confined in a very thin top layer. We also evaluated the effect on devices efficiency using both $CdSe_{495}$ and $CdSe_{545}$ QDs combined with two different dyes: the ruthenium(II) complex N719 and the metal-free TBTCA. We found a successful combination between TBTCA and $CdSe_{495}$ that resulted to increase the cell efficiency of 25%. Considerations on TCSPC experiments performed on the photoelectrode revealed FRET from $CdSe_{495}$ to TBTCA as one of the presumable mechanism, as long as IPCE curves attested that could be also a good matching of the energy levels of the entire system contributing to a better injection via electron cascade. In the case of N719 the exploited combinations are all pejorative with respect of the dye alone and the causes are not completely attributed yet.

Generally co-sensitization had been studied with the main aim to obtain an enhancement in the efficiency of the device through improved combinations of materials. Indeed in view of an actual application of this photovoltaic technology, co-sensitization would provide improvements in efficiency and stability with respect single-component system and the use of different couples of QDs and more efficient organic dyes would be a very stimulating argument for future works. Taking into account the outcomes of this work we may think that it would be possible to obtain further improvement in QDDSSCs by using organic dyes with a red shifted absorption bands, that, in the case of the TBTCA type structure, could be obtained - for example - introducing one or more thiophene units in the π-bridge and/or adding one or more electron-donating groups on the terminal phenyls of the triphenylamine unit. Additional enhancements might be obtained by using QD with modified shell having a better compatibility with the photo-anode in order to increase the amount of adsorbed particles and achieve a more effective penetration inside of the TiO_2 film. Finally the possibility to have QDs smaller than $CdSe_{495}$ might improve the mechanism of the electron transfer via cascade owing to a better separation between the CB of the TiO_2 and the LUMO of the QD.

Acknowledgements

The authors acknowledge eni S.p.A for financial support and are grateful to Ou Chen (MIT) for providing the QDs and Thomas Bischof (MIT) for TCSPC experiments.

The authors also thank Andrea Alessi and Mario Salvalaggio (eni S.p.A.) for UV-Vis Spectroscopy, Nilanjan Chatterjee (MIT) for Electron Probe Micro Analysis, Stefano Carlo Chiaberge (eni S.p.A.) for Mass Spectrometry, Elizabeth Libby Shaw (MIT) for XPS experiments, Alessandra Tacca (eni S.p.A.) for Cyclovoltammetry, Silvia Spera (eni S.p.A.) for NMR and Dong Soo Yun (MIT) for TEM characterization.

Notes and references

[a]*Department of Physical and Chemical Sciences, University of L'Aquila, via Vetoio (Coppito 1) - 67100, L'Aquila, Italy.*
[b]*Department of Chemistry, Massachusetts Institute of Technology, 77 Massachusetts Avenue, Cambridge, MA 02139, USA. E-mail: mgb@mit.edu*
[c]*Research Center for Non Conventional Energy, Istituto eni-Donegani, eni S.p.A., via Fauser, 4 - 28100, Novara, Italy. E-mail: paolo.biagini@eni.com*
[d]*Department of Chemical Engineering, Massachusetts Institute of Technology, 77 Massachusetts Avenue, Cambridge, MA 02139, USA. E-mail: hammond@MIT.edu*

† Electronic Supplementary Information (ESI) available: synthetic procedures, ^{1}H NMR and CV characterization of TBTCA; absorption and emission spectra of TBTCA, N719, $CdSe_{495}$ and $CdSe_{545}$; TEM – EDS of QDs/TiO_2 film; detailed results of XPS measurements on QDs/TiO_2 film; photovolyaic measurements and statistical analysis of all the devices prepared. See DOI: 10.1039/b000000x/

1 K. W. J. Barnham, M. Mazzer and B. Clive, *Nat. Mater.*, 2006, **5**, 161.
2 M. Jacoby, *Chem. Eng. News*, 2007, **85(35)**, 16.
3 J. -L. Bredas and J. R. Durrant, *Acc. Chem. Res.*, 2009, **42**, 1689.
4 N. Robertson, *Angew. Chem., Int. Ed.*, 2006, **45**, 2338.
5 A. Hagfeldt, G. Boschloo, L. Sun, L. Kloo and H. Pettersson, *Chem. Rev.*, 2010, **110**, 6595.
6 Md. K. Nazeeruddin, C. Klein, P. Liska and M. Graetzel, *Coord. Chem. Rev.*, 2005, **249**, 1460.
7 P. Yu, K. Zhu, A.G. Norman, S. Ferrere, A. J. Frank and A. J. Nozik, *J. Phys. Chem. B*, 2006, **110**, 25451.
8 R. Vogel, P. Hoyer and H. Weller, *J. Phys. Chem. B*, 1994, **98**, 3183.
9 I. Mora-Seró, V. Likodimos, S. Giménez, E. Martìnez-Ferrero, J. Albero, E. Palomares, A. G. Kontos, P. Falaras and J. Bisquert, *J. Phys. Chem. C*, 2010, **114**, 6755.
10 I. Mora-Seró, D. Gross, T. Mittereder, A. A. Lutich, S. Susha, T. Dittrich, A. Belaidi, R. Caballero, F. Langa, J. Bisquert and A. L. Rogach, *Small*, 2010, **2**, 221.
11 A. Mishra, M. K. Fischer and P. Bäuerle, *Angew. Chem. Int. Ed.*, 2009, **48**, 2474.
12 S. Itzhakov, S. Buhbut, E. Tauber, T. Geiger, A. Zaban and D. Oron, *Adv. Energy Mater.*, 2011, **1**, 626.
13 K. Becker, J. M. Lupton, J. Müller, A. L. Rogach, D. V. Tapalin, H. Weller and J. Feldmann, *Nat. Mater.*, 2006, **5**, 777.
14 A.J. Nozik, *Physica E*, 2002, **14**, 115.
15 J. A. McGuire, J. Joo, J. M. Pietryga, R. D. Schaller and V. I. Klimov, *Acc. Chem. Res.*, 2008, **41**, 1810.
16 M. T. Trinh, A. J. Houtepen, J. M. Schins, T. Hanrath, J. Piris, W. Knulst, A. P. L. M. Goossens and L. D. A. Siebbeles, *Nano Lett.*, 2008, **8**, 1713.
17 H. Lee, H. C. Leventis, S. -J. Moon, P. Chen, S. Ito, S. A. Haque, T. Torres, F. Nüesch, T. Geiger, S. M. Zakeeruddin, M. Grätzel and Md. K. Nazeerruddin, *Adv. Funct. Mater.*, 2009, **19**, 2735.
18 A. M. Funston, J. J. Jasienak and P. Mulvaney, *Adv. Mater.*, 2008, **20**, 4274.
19 A.Y. Koposov, P. Szymanski, T. Cardolaccia, T.J. Meyer, V.I. Klimov and V.I. Sykora, *Adv. Funct. Mater.*, 2011, **21**, 3159.
20 H. Choi, P. K. Santra and P. V. Kamat, *ACS Nano*, 2012, **6**, 5718.
21 L. Etgar, J. Park, C. Barolo, V. Lesnyak, S. K. Panda, P. Quagliotto, S. G. Hickey, Md. K. Nazeeruddin, A. A. Eychmüller, G. Viscardi and M. Grätzel, *RSC Adv.*, 2012, **2**, 2748.
22 M. Shalom, J. Albero, Z. Tachan, E. Martinez-Ferrero, A. Zaban and E. Palomares, *J. Phys. Chem. Lett.*, 2010, **1**, 1134.
23 J. Huang, D. Stockwell, Z. Huang, D. L. Mohler and T. Lian, *J. Am. Chem. Soc.*, 2008, **130**, 5632.
24 S. N. Sharma, Z. S. Pillai and P. V. Kamat, *J. Phys. Chem. B*, 2003, **107**, 10088.
25 M. Sykora, M. A. Petruska, J. Alstrum-Acevedo, I. Bezel, T. J. Meyer and V. I. Klimov, *J. Am. Chem. Soc.*, 2006, **128**, 9984.
26 Y. Liu and J. Wang, *Thin Solid Films*, 2010, **518(24)**, e54.
27 S. So, S. -Q. Fan, H. Choi, C. Kim, N. Cho, K. Song and J. Ko, *Appl. Phys. Lett.*, 2010, **97**, 263506.
28 X. Song, X. -L. Yu, Y. Xie, J. Sun, T. Ling and X. -W. Du, *Semicond. Sci. Technol.*, 2010, **25**, 095014.
29 S. -Q. Fan , R. -J. Cao, Y. -X. Xi, M. Gao, M. -D. Wang, D. -H. Kim and J. -J. Ko, *Optoelectron Adv. Mater. Rapid Commun.*, 2009, **3**, 1027.
30 H. Choi, R. Nicolaescu, S. Paek, J. Ko and P. V. Kamat, *ACS Nano*, 2011, **5**, 9238.
31 C. -A. Lin, K. P. Huang, S. T. Ho, M. –W. Huang and J. –H. He, *Appl. Phys. Lett.*, 2012, **101**, 123901.
32 V. González-Pedro, Q. Shen, V. Jovanovski, S. Giménez, R. Tena-Zaera, T. Toyoda and I. Mora-Seró, *Electr. Acta*, 2013, **100**, 35.
33 F. Guo, J. He, J. Li, W. Wu, Y. Hang and J. Hua, *J. Coll. Int. Sci.*, 2013, **408**, 59.
34 S. Paek, H. Choi, C. Kim, N. Cho, S. So, K. Song, Md. K. Nazeeruddin and J. Ko, *Chem. Commun.*, 2011, **47**, 2874.
35 M. Velusamy, K. R. J. Thomas, J. T. Lin, Y. -C. Hsu and K. -C. Ho, *Org. Lett.*, 2005, **7**, 1899.
36 D. J. Schipper and K. Fagnou, *Chem. Mater.*, 2011, **23**, 1594.
37 L. Carbone, C. Nobile, M. De Giorgi, F. Della Sala, G. Morello, P. Pompa, M. Hytch, E. Snoeck, A. Fiore, I. R. Franchini, M. Nadasan, A. F. Silvestre, L. Chiodo, S. Kudera, R. Cingolani, R. Krahne and L. Manna, *Nano Lett.*, 2007, **7**, 2942.
38 Y. J. Shen and Y. L. Lee, *Nanotechnol.*, 2008, **19**, 045602.
39 I. Mora-Seró, S. Giménez, T. Moehl, F. Fabregat-Santiago, T. Lana-Villareal, R. Gómez and J. Bisquert, *Nanotechnol.*, 2008, **19**, 424007.
40 J. Chen, J. L. Song, X. W. Sun, W. Q. Deng, C. Y. Jiang, W. Lei, J. H. Huang and R. S. Liu, *Appl. Phys. Lett.*, 2009, **94**, 153115.
41 I. Robel, V. Subramanian, M. Kuno and P. V. Kamat, *J. Am. Chem. Soc.*, **128**, 2385.
42 N. Guijarro, T. Lana-Villareal, I. Mora-Seró, J. Bisquert and R. Gómez, *J. Phys. Chem. C*, 2009, **113**, 4208.
43 S. Rühle, M. Shalom and A. Zaban, *Chem. Phys. Chem.*, 2010, **11**, 2290.
44 W. W. Yu, L. Qu, W. Guo and X. Peng, *Chem. Mater.*, 2003, **15**, 2854.
45 S. J. B. Reed, *Electron microprobe analysis,* 2nd Ed., Cambridge University Press, Cambridge, 1993.
46 S. Ito, T. N. Murakami, P. Comte, P. Liska, C. Grätzel, Md. K. Nazeeruddin and M. Grätzel, *Thin Solid Films*, 2008, **516**, 4613.
47 V. González-Pedro, Q. Shen, V. Jovanovski, S. Giménez, R. Tena-Zaera, T. Toyoda and I. Mora-Seró, *Electrochim. Acta*, 2013, **100**, 35.
48 Y. Gao, X. Zou, Z. Sun, Z. Huang and H. Zhou *J. Nanomater.*, 2012, 415370.
49 H. Shen, H. Lin, Y. Liu, J. Li and D. Oron, *J. Phys. Chem. C*, 2012, **116**, 15185.

50 H. Choi and P.V. Kamat *J. Phys. Chem. Lett.,* 2013, **4**, 3983.

51 C. -F. Chi, H. -W. Cho, H. Teng, C. -Y. Chuang, Y. –M. Chang, Y. -J. Hsu and Y. -L. Lee, *Appl. Phys. Lett.*, 2011, **98**, 012101.

52 F. Lenzmann, J. Krueger, S. Burnside, K. Brooks, M. Grätzel, D. Gal, S. Rühle and D. Cahen, *J. Phys. Chem. B*, 2001, **105**, 6347.

53 C. J. Murphy and J. L. Coffer, *Appl. Spectr.,* 2002, **56**, 16A.

Enhanced Photovoltaic Performance with Co-Sensitization of Quantum Dots and an Organic Dye in Dye-Sensitized Solar Cells

Camilla Lelii, Moungi G. Bawendi,* Paolo Biagini,* Po-Yen Chen, Marcello Crucianelli, Julio M. D'Arcy, Francesco De Angelis, Paula T. Hammond,* and Riccardo Po

Four novel hybrid CdSe quantum-dots/organic dye materials for dye-sensitized solar cells are presented. The enhancement of the efficiency in the hybrid devices depends on the size of the quantum dot and on the nature of the dye.